

# Supporting Information

## Gambrill and Barria 10.1073/pnas.1012676108

### SI Materials and Methods

**Constructs.** EGFP-tagged NMDAR subunits were cloned in pCI plasmid (Promega) and described previously (1). Chimeric NR2 subunits NR2A-CTB and NR2B-CTA were constructed by amplifying the entire C terminus from residue L797 in NR2A and amino acid L793 in NR2B and adding a Kpn1 and Xho1 restriction site at the 5' end of the NR2A and NR2B PCR products respectively. A second PCR fragment was amplified from the endogenously occurring Kpn1 site in NR2A and Sph1 in NR2B to position L797 or L793 with a Kpn1 or Xho1 restriction site at the 3' end. These two PCR fragments were subcloned into the corresponding pCI-EGP-NR2 subunit.

**siRNA.** Endogenous NR2A and NR2B subunits were knocked down using the pSuper RNAi system from Oligoengine, a mammalian expression vector that directs intracellular synthesis of siRNA-like transcripts. Preliminary data were collected using pSuper plasmids obtained from Morgan Sheng (Genentech, South San Francisco, CA) and described previously (2). Subsequently, we cloned the same target sequence into pSuper.gfp/neo (Oligoengine; VEC-PBS-0006) to take advantage of eGFP coexpression with the desired siRNA. Empty vector and scrambled siRNA were used as controls.

**Fixed Imaging.** CA1 neurons were imaged on an Olympus FV confocal laser scanning microscope with an Olympus 60 $\times$  objective (N.A. 1.10). Successful expression of mCherry-tagged NMDARs was confirmed using epifluorescence. Dendrites were imaged using the green channel with 0.5- $\mu$ M steps in the z axis. Each

optical plane was averaged two or three times (Kalman filter). Image analysis was done using ImageJ version 1.4.

**Live Cell Imaging.** For motility experiments, transfected slices were perfused with artificial cerebrospinal fluid constantly gassed with 5%CO<sub>2</sub>/95%O<sub>2</sub>. Temperature in the imaging chamber was held at 34 °C. A section of dendrite was repeatedly imaged as described every 10 min for 120 min. For each cell, one to two sections of dendrite were imaged. For imaging experiments where eGFP was used as a cytosolic marker, the eGFP tag in NMDAR subunits was replaced with mCherry.

**Analysis of Spines.** Images were analyzed using ImageJ. A total dendritic length of 160–1,000  $\mu$ m, consisting of the primary apical dendrite and secondary branches, was analyzed per cell. Spines were defined as protrusions more than 0.5  $\mu$ m and less than 3  $\mu$ m long and with a round head. A region of interest (ROI) was drawn around the selected spine. Mean fluorescent intensity in each plane of the Z-stack containing the spine was calculated (S), background subtracted (B), and summed. A ROI of equal size was drawn on the dendrite adjacent to the spine, and the mean fluorescent intensity of each plane was calculated (D), background subtracted (B), and the average of these values taken. Spine fluorescence was normalized by dendrite fluorescence. Volume index =  $\Sigma(S_n - B_n) / (\Sigma(D_n - B_n) / N)$ . For motility analysis, spines visible in the first image were marked and events in subsequent images counted. Events were defined as the loss of an existing spine, the emergence of a new spine, and the appearance or extension of filopodia. Filopodia were defined as protrusions over 3  $\mu$ m in length, with no visible head.

1. Barria A, Malinow R (2002) Subunit-specific NMDA receptor trafficking to synapses. *Neuron* 35:345–353.
2. Kim MJ, Dunah AW, Wang YT, Sheng M (2005) Differential roles of NR2A- and NR2B-containing NMDA receptors in Ras-ERK signaling and AMPA receptor trafficking. *Neuron* 46:745–760.



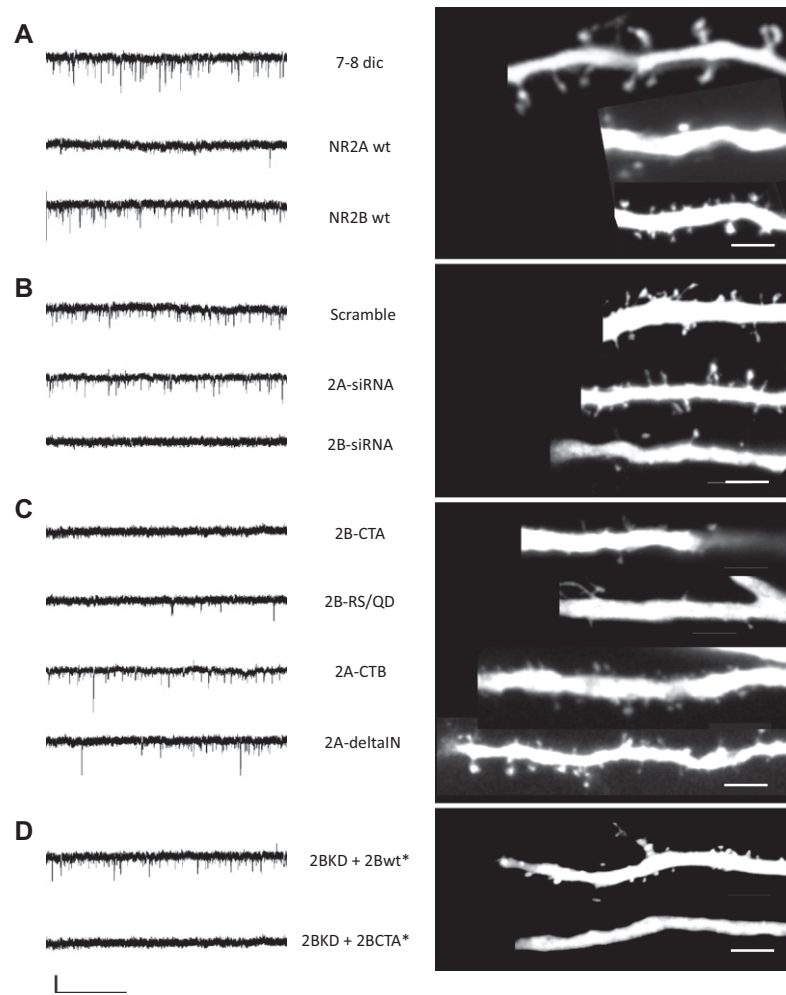


**Fig. S2.** Spine density imaging examples and mEPSC traces. (A) Examples from nontransfected cells 7–8 dic (*Top*), cell of equivalent age-expressing NR2A WT (*Middle*) or NR2B WT (*Bottom*). (B) Examples from cells expressing scrambled siRNA (*Top*), 2A siRNA (*Middle*), or 2B siRNA (*Bottom*); compared in the text to nontransfected 7–8 dic cells (A). (C) Examples from cells expressing 2B-CTA (*Top*), 2B-RS/QD (second from *Top*), 2A-CTB (second from *Bottom*), or 2A $\Delta$ IN (*Bottom*); compared in text to 7–8 dic nontransfected, NR2A WT-, and NR2B WT-expressing cells (A). (D) Examples from cells expressing 2B siRNA and 2B\* (resistant to knockdown) WT (*Upper*) or 2B-CTA\* (*Lower*); compared in text to cells expressing 2B siRNA alone (B) and 7–8 dic nontransfected (A). (mEPSC trace scale bar, 20 pA and 1.3 s; spine density imaging scale bar, 5  $\mu$ m.)

**Table S1. Student *t* test *P* values**

Figure	Variable	Cond 1	Cond 2	<i>P</i> value
Fig. 1C	Spine density	4–5 dic	7–8 dic	0.0000
	Spine density	7–8 dic	11–12 dic	0.7728
Fig. 1D	Total motility	4–5 dic	7–8 dic	0.6898
	Total motility	7–8 dic	11–12 dic	0.0012
Fig. 1E	Filopodia	4–5 dic	7–8 dic	0.1138
	Filopodia	7–8 dic	11–12 dic	0.0154
Fig. 1F	Additions	4–5 dic	7–8 dic	0.4393
	Additions	7–8 dic	11–12 dic	0.0178
Fig. 1G	Retractions	4–5 dic	7–8 dic	0.2476
	Retractions	7–8 dic	11–12 dic	0.0274
Fig. 2B	Spine density	7–8 dic	2A	0.0081
	Spine density	7–8 dic	2B	0.7874
Fig. 2C	Total motility	7–8 dic	2A	0.0470
	Total motility	7–8 dic	2B	0.0170
Fig. 2D	Filopodia	7–8 dic	2A	0.0810
	Filopodia	7–8 dic	2B	0.3594
Fig. 2E	Additions	7–8 dic	2A	0.0388
	Additions	7–8 dic	2B	0.0370
Fig. 2F	Retractions	7–8 dic	2A	0.4035
	Retractions	7–8 dic	2B	0.0328
Fig. 2G	Spine volume	4–5 dic	7–8 dic	0.2724
	Spine volume	7–8 dic	11–12 dic	0.4566
	Spine volume	7–8 dic	2A	0.019
	Spine volume	7–8 dic	2B	0.7157
Fig. 3A	EPSCs peak amplitude	Control NT	2B KD	0.0041
	EPSCs peak amplitude	Control NT	2A KD	0.3528
Fig. 3B	THD	Control NT	2B KD	0.0300
	THD	Control NT	2A KD	0.0308
Fig. 4B	Spine density	7–8 dic	Scrambled	0.6754
	Spine density	7–8 dic	2B KD	0.0074
	Spine density	7–8 dic	2A KD	0.2360
Fig. 4C	Total motility	7–8 dic	Scrambled	0.9027
	Total motility	7–8 dic	2B KD	0.0021
	Total motility	7–8 dic	2A KD	0.1840
Fig. 4D	Filopodia	7–8 dic	Scrambled	0.1475
	Filopodia	7–8 dic	2B KD	0.0062
	Filopodia	7–8 dic	2A KD	0.5496
Fig. 4E	Additions	7–8 dic	Scrambled	0.8056
	Additions	7–8 dic	2B KD	0.0462
	Additions	7–8 dic	2A KD	0.3647
Fig. 4F	Retractions	7–8 dic	Scrambled	0.4609
	Retractions	7–8 dic	2B KD	0.4428
	Retractions	7–8 dic	2A KD	0.1909
Fig. 5A	Spine density	7–8 dic	2A	0.0081
	Spine density	7–8 dic	2BCTA	0.0354
	Spine density	7–8 dic	2BRSQD	0.0446
Fig. 5C	Spine density	7–8 dic	2B	0.7874
	Spine density	7–8 dic	2ACTB	0.7551
	Spine density	7–8 dic	2AΔIN	0.8732
Fig. 5E	Spine volume	7–8 dic	2A	0.019
	Spine volume	7–8 dic	2BCTA	0.036
	Spine volume	7–8 dic	2BRSQD	0.008
Fig. 5F	Spine volume	7–8 dic	2B	0.7157
	Spine volume	7–8 dic	2ACTB	0.5770
	Spine volume	7–8 dic	2AΔIN	0.1220
Fig. 6B	Spine density	7–8 dic	2B KD	0.0074
	Spine density	7–8 dic	2BKD + 2B*	0.3321
	Spine density	7–8 dic	2BKD + CTA*	0.0187